Small-Angle Orientational Motions of Spin-Labeled Lipids in Cholesterol-Containing Bilayers Studied at Low Temperatures by Electron Spin Echo Spectroscopy

Nikolay P. Isaev,[†] Victoria N. Syryamina,[‡] and Sergei A. Dzuba*[,†,‡]

Institute of Chemical Kinetics and Combustion, Institutskaya-3, 630090 Novosibirsk, Russia, and, Novosibirsk State University, 630090, Pirogova-2, Novosibirsk, Russia

Received: May 14, 2010; Revised Manuscript Received: June 22, 2010

Electron spin echo (ESE) study was performed for a 1-palmitoyl-2-oleoyl-*sn*-glycero-3-phosphocholine (POPC) bilayer containing an admixture of lipids (of 1:100 molar ratio) spin-labeled at the polar head or at different positions along the acyl chain and optionally containing additionally cholesterol that substituted POPC lipids in a 50:50 molar ratio. ESE signal was observed below 150−115 K, depending on the label position. Three-pulse stimulated ESE is sensitive to two types of orientational motion of spin labels at these temperatures. The first type of motion (which is also seen in a two-pulse primary ESE experiment) is fast stochastic librations, with a correlation time in the nanosecond scale. The second type of motion is slow millisecond rotations, which in the accessible microsecond time scale are seen as small-angle reorientations. (Restricted rotations also refer to this type of motion.) We found that in presence of cholesterol, fast librations are enhanced at all label positions. This effect may be related to the cholesterol ordering effect. Rotational motions in the presence of cholesterol are remarkably suppressed near the bilayer surface, which may be readily explained by the cholesterol condensing effect. In contrast to that, in the bilayer center rotations in the presence of cholesterol are remarkably enhanced. This effect may be attributed to topological properties of a cholesterol-containing membrane system in which beyond the steroid core, more freedom appears for small-angle motions, as compared with the cholesterol-free case. The found property may be important for physiological temperatures, as well. In particular, it may imply that cholesterol weakens interaction between two leaflets in the bilayer.

Introduction

Cholesterol is known to increase the mechanical stability of cell membranes,[1−4] to increase order of phospholipids acyl chains (ordering effect),[5−8] to decrease the surface area per lipid (condensing effect),[8−11] to promote formation of lipid rafts,[12,13] to suppress lateral diffusion of lipids and proteins in membranes,[8,14] and to influence some other important properties of membranes. However, at the molecular level, the action of cholesterol is still not satisfactorily understood.

Among a large variety of experimental approaches for studying biological membranes at the molecular level, electron paramagnetic resonance (EPR) of spin labels is also used (see, e.g., refs 15−17 and references therein). Normally, EPR is applied at physiological temperatures. However, at these temperatures, different types of motion exist (internal, overall, segmental, collective, etc.), which essentially complicates analysis of the experimental data. Meanwhile, study of molecular motions at low (cryogenic) temperatures may help selection of different motional mechanisms. As has been recently shown,[18−20] pulsed EPR in a version of stimulated three-pulse electron spin echo (ESE) technique applied to spin labels enables at low temperatures a direct observation of two types of molecular motion. The first type of motion (which is also seen in a two-pulse primary ESE experiment) is fast stochastic molecular librations (i.e., stochastic orientational oscillations of molecules), with correlation time on a scale of nanoseconds. The second type of motion is slow millisecond inertial rotations, which in the accessible microsecond time scale are seen as small-angle reorientations, by angles on the order of 1° (highly restricted rotations also refer to this type of motion). The advantage of the stimulated ESE technique is that interpretation of results does not require theoretical simulation or attraction of sophisticated motional models.

For 1-palmitoyl-2-oleoyl-*sn*-glycero-3-phosphocholine (POPC) bilayers, an echo signal from the spin labels is observed below ∼150 K.[18,20] At higher temperatures, it decays too fast because of spin relaxation. In the previous stimulated ESE study of the influence of cholesterol on molecular motions,[20] the system of spin-labeled lipid 1-palmitoyl-2-stearoyl-(5-doxyl)-*sn*-glycero-3-phosphocholine (5-PCSL) embedded in a POPC bilayer was employed. The presence of cholesterol in lipid bilayers was found to suppress remarkably rotational motions, whereas stochastic librations, in the contrast, seem to become somewhat enhanced. These results were discussed in the relation with the known condensing and ordering effects of cholesterol.

In this work, we study the influence of cholesterol in multilamellar POPC bilayers (frozen to a gel phase) on molecular motions of lipids spin-labeled at the polar head and at different positions along the acyl carbon chain. In combination with previous data on 5-PCSL,[20] the results allow getting more detailed information on the influence of cholesterol on molecular motions in model membranes.

Experimental Section

Sample Preparations. To prepare lipid bilayers, phospholipids POPC

* Corresponding author. Fax: +7(383) 330 7350. E-mail: dzuba@ns.kinetics.nsc.ru.
[†] Institutskaya-3.
[‡] Novosibirsk State University.

10.1021/jp1043927
Published on Web 07/08/2010

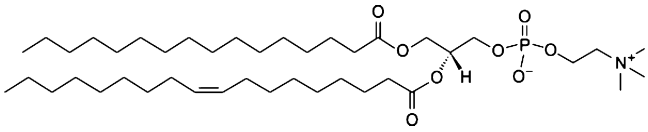

(Aldrich) were employed. Spin-labeled lipid 1-palmitoyl-2-oleoyl-*sn*-glycero-3-phospho(*tempo*)choline (T-PCSL)],

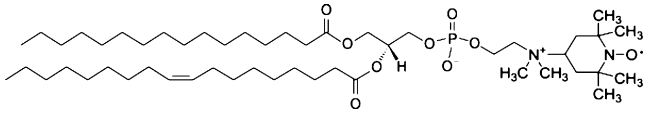

1-palmitoyl-2-stearoyl-(10-doxyl)-*sn*-glycero-3-phosphocholine (10-PCSL),

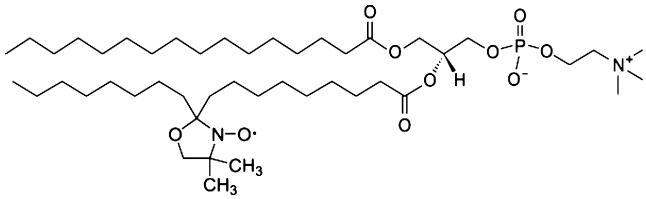

and 1-palmitoyl-2-stearoyl-(16-doxyl)-sn-glycero-3-phosphocholine (16-PCSL)

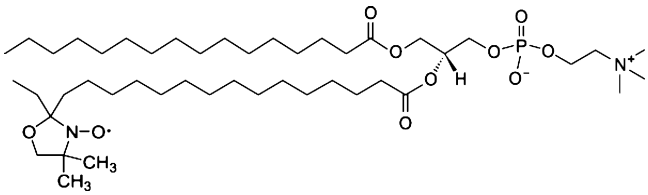

were used (Avanti). In addition, in sample preparations, cholesterol

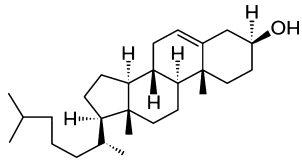

(Avanti) was used. For each of the spin-labeled lipids, two types of samples were prepared: mixture with POPC at a 1:100 molar ratio (cholesterol-free sample), and a mixture with POPC and cholesterol at a 1:50:50 molar ratio (cholesterol-containing sample). These mixtures were dissolved in chloroform. Then the solvent was removed by nitrogen flow and evaporation, followed by a few hours under vacuum. Then twice-distilled water was added, and the samples were stored at room temperature for 24 h. The samples were then centrifuged for an hour, followed by removal of the excess water. The final total water content in the sample was around 50% w/w.

EPR Measurements. A Bruker Elexsys E580 X-band FT EPR spectrometer equipped with a dielectric cavity (Bruker ER 4118 X-MD-5) inside an Oxford Instruments CF 935 cryostat was used. Duration of microwave pulses in a 3-pulse stimulated echo sequence $\pi/2-\tau-\pi/2-T-\pi/2-\tau-$echo was 16 ns. The pulse amplitudes were adjusted to provide a $\pi/2$ turning angle, thus making the amplitude ~6 G (that is, the excitation bandwidth). The cryostat was cooled either by cold nitrogen gas or by cold helium gas. The sample temperature was monitored with a calibrated Cu-constantan thermocouple directly placed into the sample tube. The temperature was maintained with an accuracy of ±0.5 K.

Data Analysis. For a nitroxide spin label experiencing fast stochastic librations around the X molecular axis, when the reorientation angle is small, $\alpha(t) \ll 1$, the echo signal decays as[18,19,21]

$$E_{\text{fast}}(2\tau, T) \propto \exp\left(-2 < \alpha(t)^2 > R_X^2(\theta, \varphi)\tau\tau_c\right) \qquad (1)$$

where

$$R_X(\theta, \varphi) = \gamma\left[B(g_{YY} - g_{ZZ}) + \frac{m(A_{YY}^2 - A_{ZZ}^2)}{(A_{XX}^2 \sin^2\theta\cos^2\varphi + A_{YY}^2 \sin^2\theta \sin^2\varphi + A_{ZZ}^2 \cos^2\theta)^{1/2}}\right] \times \cos\theta \sin\theta \sin\varphi$$

and where γ is the gyromagnetic ratio; τ_c is the correlation time for motion; θ and φ are angles determining the orientation of the magnetic field in the molecular framework; B is the magnetic field strength; g_{YY}, g_{ZZ}, A_{YY}, and A_{ZZ} are principal values of the **g** tensor and the tensor of hyperfine interaction; and m is the nitrogen nucleus spin projection onto its quantization axis ($m = 0, \pm 1$). Fast motion means that $R_X^2(\theta, \varphi)\tau_c^2 < 1$. As for nitroxides at the X-band microwave frequency, the maximum $R_X(\theta, \varphi)$ value attains a magnitude of $\sim 3 \times 10^8$ s^{-1} (see also below), this condition means that τ_c lies at the nanosecond time scale. For a small-amplitude motion, angles θ and φ in eq 1 may be considered as constants. When studying the relaxation within a particular hyperfine structure component, m also may be taken as a constant. (Normally the assumption that m is constant allows us to fit well echo-detected EPR spectra.[21]) For motion around the two other molecular axes, Y and Z, a circular permutation in eq 1 has to be made of the subscripts X, Y, Z simultaneously with polar coordinates sin θ cos φ, sin θ sin φ, and cos θ.

The second type of motion is slow millisecond rotations. For the model of slow inertial rotations, in which the molecule freely rotates around the X molecular axis with an angular velocity, Ω, during the experimental time interval (for different molecules Ω may be different), the echo decays as[18,19]

$$E_{\text{slow}}(2\tau, T) \approx \exp\left(-|R_X(\theta, \varphi)|\Omega_X(\tau^2 + \tau T)\right) \qquad (2)$$

where Ω_X is a parameter characterizing the width of the distribution function for the angular velocities for motion around X. In the case of a Lorentzian distribution, Ω_X corresponds to the half width at the half height of this distribution.

Both mechanisms given by eqs 1 and 2 result in an exponential decay when τ is varied. The rates of the decay for these mechanisms are given by formulas

$$W_{\text{fast}}^X(T) = 2 < \alpha(t)^2 > R_X^2(\theta, \varphi)\, \tau_c \qquad (3a)$$

and

$$W^X_{\text{slow}}(T) = |R_X(\theta, \varphi)|\Omega_X T \quad (3b)$$

respectively. In the latter case, it is taken into account that in a three-pulse stimulated echo experiment, normally, $T \gg \tau$ (cf. eq 2).

Note that for fast motion, $W(T)$ does not depend on T, but for slow motion, it depends linearly. The result for the former case has a simple physical meaning: for fast motions $\tau_c \ll \tau$, so evolutions of magnetization during the two τ-intervals are statistically independent.

Normally, an assumption of isotropic motion is employed for small-angle molecular motion of spin labels in disordered systems[19] and in bilayers,[22−24] which assumes that motion occurs independently around all three molecular axes. This model implies that total relaxation rate instead of 3 is

$$W_{\text{fast}}(T) = W^X_{\text{fast}}(T) + W^Y_{\text{fast}}(T) + W^Z_{\text{fast}}(T) \quad (4a)$$

and

$$W_{\text{slow}}(T) = W^X_{\text{slow}}(T) + W^Y_{\text{slow}}(T) + W^Z_{\text{slow}}(T) \quad (4b)$$

with motional parameters $\langle\alpha(t)^2\rangle\tau_c$ and $\Omega_{X(Y,Z)}$ being equal for motions around all three molecular axes.

Results

The EPR spectrum of nitroxides consists of three hyperfine components because the projection m of the nitrogen spin ($I = 1$) on its quantization axis acquires three values, $m = 0, \pm 1$. Figure 1 presents continuous wave (CW) EPR spectra taken at room temperature for the samples investigated in this work. The spectral shapes are in agreement with those published in the literature.[16]

The echo signal recorded at 77 K as a function of scanning magnetic field results in a so-called echo-detected spectrum (see the insert to Figure 2a). The middle component in the spectrum is the narrowest one, because only anisotropy of the **g** tensor here matters. The high-field component is the most anisotropic and so the broadest one. Position 1 in the spectrum corresponds to the largest anisotropy of the ensemble of contributing spins, whereas position 2 corresponds to the smallest anisotropy.

The echo decays given in Figure 2a as a function of τ show that larger anisotropy results in a faster decay, which implies that spin relaxation induced by orientational motion of the spin label does contribute to the echo decay. Note that in organic solids, a major contribution to the echo decay arises because of spin relaxation induced by fluctuating electron−nuclear spin interactions of the unpaired electron with surrounding protons in the matrix. These interactions fluctuate because of spin diffusion in the nuclear subsystem or because of molecular motion of atomic groups containing protons. In addition, static electron−nuclear interactions induce noticeable oscillations on the decay curves that are clearly seen in Figure 2a (a so-called electron spin echo envelope modulation, or ESEEM).

We suggest that echo decay induced by orientational motion of the spin labels occurs independent of the decays induced by other contributions to spin relaxation and that these other contributions are field-independent in the field range of the nitroxide EPR spectrum. Therefore, we may refine the pure contribution of the decay induced by orientational motion by dividing numerically the time traces for the first field position

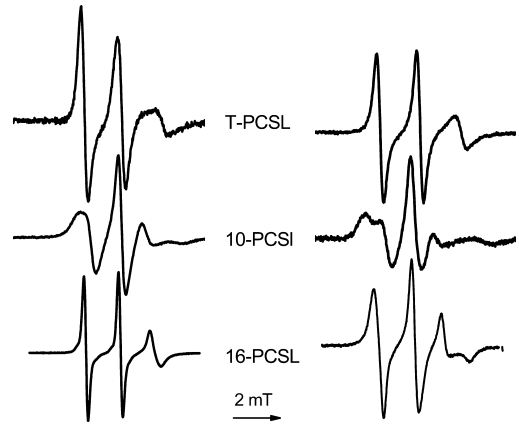

Figure 1. Room temperature EPR spectra of POPC bilayers containing spin labeled lipids in a 1:100 molar ratio. Left, cholesterol-free samples; right, cholesterol-containing samples (50:50 cholesterol/lipid molar ratio).

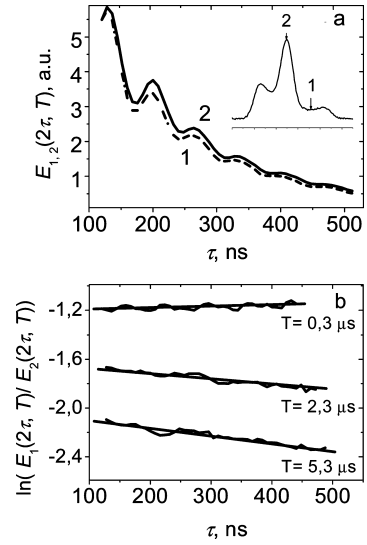

Figure 2. (a) Echo decay traces vs τ for $T = 0.3$ μs for two field positions shown in the insert, where the echo-detected EPR line shape is given. The intensities at the beginning are artificially adjusted to approximately the same value. (b) Semilogarithmic plot of the ratio of the traces taken at positions 1 and 2 for different time delays, T, shown in the picture. The straight lines are linear approximations of these data. For convenience, data are shifted arbitrarily along the vertical axis. Temperature is 112 K, sample is 10-PCSL for a cholesterol-free POPC bilayer preparation.

by those for the second one. The results are given in a semilogarithmic scale in Figure 2b for three different T delays. Note that after this division, ESEEM is virtually canceled, which means that it is field-independent.

One can see in Figure 2b that echo decays are satisfactorily fitted by straight lines, which implies that decays are exponential. Thus, we may introduce the slopes of these lines as parameters having a clear meaning in the simple theory presented by eqs 1−4. Hereafter, we denote these experimentally obtained parameters as $W(T)$.

From the data like those presented in Figure 2b, we estimate that experimental uncertainty in measurements of $W(T)$ consists of two components: the absolute one that is about ± 0.05 μs^{-1} and the relative one that is about $\pm 0.08W(T)$.

Figure 3 shows $W(T)$ values vs T for samples containing T-PCSL, 10-PCSL, and 16-PCSL in cholesterol-free (left panel in Figure 3) and cholesterol-containing (right panel) POPC bilayers preparations and at different temperatures. One can see

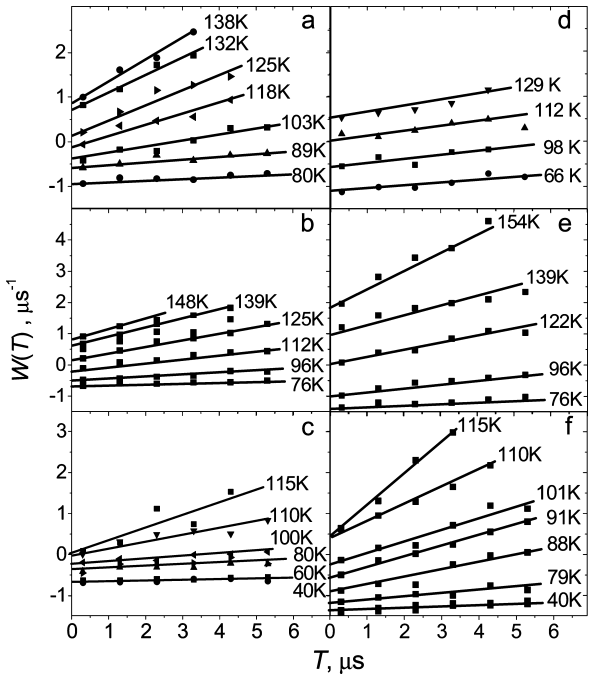

Figure 3. Relaxation rates $W(T)$ vs T obtained from the slopes of the straight lines, like those shown in Figure 2b. Left panel (a, b, c), cholesterol-free POPC bilayer; right panel (d, e, f), cholesterol-containing POPC bilayer. (a, d) T-PCSL, (b, e) 10-PCSL, (c, f) 16-PCSL.

that all data in Figure 3 can be satisfactorily approximated by straight lines, with the intercepts at $T = 0$ increasing with temperature.

The negative $W(T)$ intercepts at $T = 0$ seen in Figure 3 may be readily explained by a so-called instantaneous diffusion process in ESE. This process is induced by alternation of the sign of the dipole−dipole interaction between different spin labels under the action of the microwave pulses. For nitroxide spin labels, the influence of the instantaneous diffusion process was quantitatively described previously.[25] The rate of the additional echo decay due to this process depends on the label concentration and is proportional to the fraction of excited spins. The latter is highest for the excitation of the central component (position 2 in Figure 2a), which does explain the appearance of the negative $W(T)$ values. It is important to note that the rate of the decay due to this mechanism is temperature-independent, thus presenting a sole contribution to $W(T)$ at low temperatures where motion is absent.

For samples with different label position, the temperatures where ESE signal could be observed are also different, varying from ~154 K for 10-PCSL to ~115 K for 16-PCSL. The same effect was found previously for POPC bilayer with embedded stearic acid spin-labeled at different positions along the acyl chain.[18] It was interpreted as a consequence of heterogeneity of molecular motions across the bilayer. Note that, as was mentioned above, echo decays are due not only to molecular motion of the spin label itself but also to the motion of neighboring atomic groups containing magnetic nuclei (protons).

Discussion

The spectral line shape seen in CW EPR (Figure 1) at room temperature is determined by nanosecond large-amplitude reorientational motion.[16] According to the analysis made in the literature (see, e.g., ref 16), addition of cholesterol (cf. spectra in the right and left columns in Figure 1) results in increasing molecular order so that motion becomes geometrically more restricted and increases the reorientation correlation time. Both the order and correlation time decrease with increasing n position along the acyl chain.[16]

Experimental data presented in Figure 2b show an exponential behavior when τ is varied, which may be readily explained by eqs 1 or 2. To explain both linear T-dependences and temperature-dependent intercepts at $T = 0$ seen in Figure 3, multiplication of both of these equations must be applied.[18−20] This may take place if spin labels participate simultaneously in fast stochastic librations and in slow rotations. Therefore, the experimentally found $W(T)$ rates are to be compared with the sum (see eqs 3 and 4)

$$W(T) = W_{\text{fast}}(T) + W_{\text{slow}}(T) \tag{5}$$

The first term in 5 determines the initial intercept (along with the temperature-independent contribution from the instantaneous diffusion; see above), and the second one describes the linear T-dependence.

For cholesterol-containing samples, $W(T)$ values at low temperatures are shifted down to negative values, as compared with the cholesterol-free samples (cf. left and right panels in Figure 3). At low temperatures, the $W(T)$ rates are determined mostly by instantaneous diffusion, so this shift means that the local spin concentration (that is important for the instantaneous diffusion mechanism) is higher in the presence of cholesterol. An increase in the spin concentration may be readily explained by the cholesterol condensing effect. This increase is rather slight because it does not induce a noticeable line broadening in CW EPR spectra (see Figure 1; the instantaneous diffusion mechanism in ESE, as compared with CW EPR line shape, is sensitive to concentrations one or two orders smaller).

A slight nonzero value of the line slopes in Figure 3d most likely is not related with motion because it does not depend on temperature. The possible explanation here is the destroying of instantaneous diffusion by mutual spin flips due to spin diffusion in the system of electron spins[26] (which is temperature-independent).

Previously,[18,19] it was shown that under the used experimental setup, the $|R_X(\theta, \varphi)|$ and $|R_Y(\theta, \varphi)|$ values in eqs 1 and 2 may be safely replaced by a constant equal to 2.8×10^8 s^{-1}. As for nitroxides $|R_{X(Y)}(\theta, \varphi)| > > |R_Z(\theta, \varphi)|$, the latter value for rough estimations may be neglected. Thus, from data in Figure 3, using eqs 3, motional parameters may be obtained. (For correct experimental determination of $W(T)$ values, one must exclude the influence of instantaneous diffusion. For that purpose, the found $W(T)$ value is to be subtracted by a corresponding value obtained at a temperature low enough so that motion is frozen out.)

In addition, in our model, only motions around the X and Y axes matter for relaxation (with equal contributions for two axes). Taking into account eqs 4 and to obtain total motional parameters for motion around all 3 axes, experimental data on $W(T)$ are multiplied by a factor of 1.5 (i.e., total rotational rate $\Omega_0 = \Omega_X + \Omega_Y + \Omega_Z$). The results are given in Figure 4 in an Arrhenius plot for different samples studied. Here, data on the 5-PCSL sample calculated from the results presented in ref 20 also are given.

Note that the obtained Ω_0 value lies between the limits of $\sim 3 \times 10^2$ and $\sim 3 \times 10^3$ s^{-1} (see Figure 4). If we multiply these limits by the time scale of the experiment (5×10^{-6} s, see Figure 3), we obtain that observed characteristic angle of reorientation in slow rotations is around 0.1−1°.

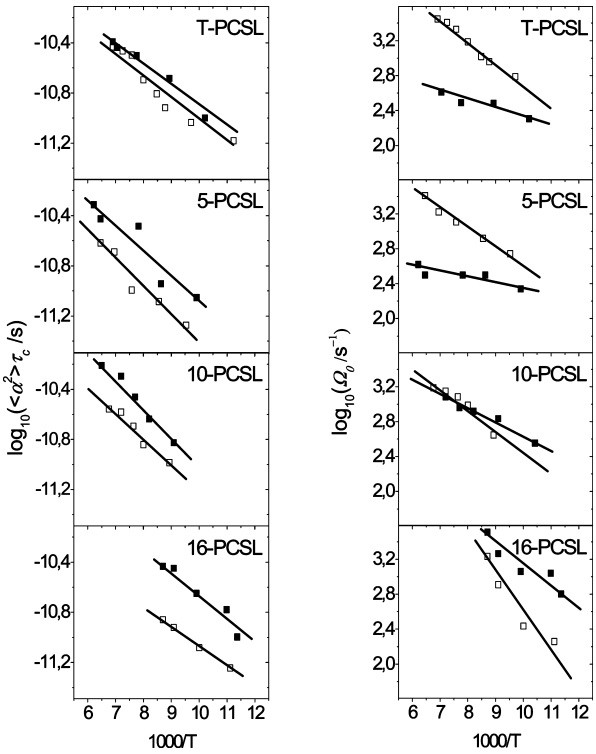

Figure 4. Arrhenius plot of the motional parameters (see text) obtained for fast motion (left panel) and for slow motion (right panel). Empty squares, cholesterol-free samples; solid squares, cholesterol-containing samples. Data for 5-PCSL are obtained from analysis of results presented in ref 20.

The results given in Figure 4 show that the presence of cholesterol has a different impact for different label positions. In addition, it influences librational and rotational motions in a different ways. For the position in the polar lipid head, cholesterol slightly increases the intensity of fast librations and strongly suppresses slow rotations. The analogous situation takes place for fifth carbon position in the acyl chain.[20] For the 10th carbon position, the situation changes: cholesterol increases the intensity of both fast librations and slow rotations, and for the 16th carbon position (i.e., in the bilayer center), cholesterol enhances both types of motion remarkably.

The observed cholesterol-induced enhancement of librational motion may be readily explained on the basis of the cholesterol-ordering effect.[5−8] This effect implies that lipid molecules are less mutually entangled, so librations may be facilitated. The suppression of rotational motions for positions near the polar head (including the fifth carbon position in acyl chain) may be related to the condensing effect of cholesterol,[8−11] which imply that the "global" structure of the bilayer in the presence of cholesterol becomes stiffer.

To our knowledge, the effect of cholesterol-induced enhancement of motions in the bilayer center has not previously been reported in the literature, despite quite a lot of data on molecular motions in membranes. ^{2}H NMR studies[27] showed that cholesterol does not noticeably influence the rates of trans−gauche isomerization of lipid chains in the bilayer center (both in the fluid and gel phases). High-field EPR on spin-labeled lipids[15] showed that total reorientation angles in the bilayer center are nearly the same in the presence and the absence of cholesterol (both in the fluid and gel phases). The known structural data also at first glance does not support the suggestion of enhancement of motion in the bilayer center: in ^{2}H NMR studies of model phospholipids bilayers[28] (in the fluid phase), it was found that cholesterol increases the molecular order at all the positions along the lipid chain. However, some data available in the literature nevertheless are in favor of the effect found here: EPR studies[16] have showed that reorientational correlation times for *n*-PCSL at room temperature, for $n < 14$ in the presence of cholesterol essentially larger than in its absence and for $n = 16$, became equal in both these cases.

We suppose that the effect of the cholesterol-induced enhancement of lipid motion in the bilayer center observed here appears because of the specificity of the motions seen by ESE. As was mentioned above, stimulated ESE reports on the motions developing within very small range of angles, around ∼1°. Such small-amplitude reorientations cannot be detected by other experimental techniques, such as CW EPR or ^{2}H NMR, and the observed enhancement may be explained as a natural consequence of the fact that a bulky steroid nucleus does not influence lipid ordering beyond its location; that is, in the bilayer center.[29] Therefore, in the bilayer center, more freedom may exist for the small-angle motion.

Near the 10th carbon position, according to known membrane topology,[15,30] the steroid nucleus ends, so the picture is intermediate between the fifth and 16th positions (see Figure 4).

Because the suggested explanation is based on the topological properties only, one may expect this cholesterol-induced enhancement of motion to take place also at physiological temperatures. However, this suggestion needs confirmation by application of other experimental techniques. In addition, comparison of lipid bilayers at the fluid and deeply frozen states must be done with caution.

One of the consequences that could follow from the found enhancement is that the mutual entanglement of lipids of the two opposite leaflets of the membrane (in other words, interdigitation of the lipids) in the presence of cholesterol becomes weaker. This effect may contribute to the total thickening of the membranes by cholesterol addition that is known from numerous X-ray studies.[16,31−36] Interleaflet coupling in bilayers is known to be important for various their properties;[37−39] however, the role of cholesterol in this coupling is still debated.[39]

Conclusions

Three-pulse stimulated ESE applied to spin labels is sensitive to fast stochastic librations, with a correlation time on the nanosecond scale (this type of motion is also seen in a two-pulse primary ESE experiment), and to slow millisecond rotations developing in the experimentally accessible microsecond time scale within a small angular range, by angles on the order of 1°.[18,19] For such small angles, it is not important which type of motion takes place, overall or segmental, and motion may be considered as isotropic.

The approach does not require complicated theoretical simulations. Moreover, the knowledge of the precise values of the *g* factor and hyperfine interaction tensors also is not important. (Even a rather crude approximation of axial isotropy of the **g** tensor may be safely applied.[18−20])

Because the echo signal experiences fast relaxation at ambient temperatures, in the studied system, it may be observed at cryogenic temperatures only. From the other side, the study of molecular motions at low temperatures may help to select different types of motion.

Data obtained in this work show that cholesterol enhances fast librations everywhere in the bilayer, which may be attributed to the known ordering effect. Cholesterol also remarkably influences small-amplitude slow rotations. However, it acts in

an opposite way near the bilayer surface and in the bilayer center. In the former case, the presence of cholesterol suppresses rotational motion. This result may be related to the known condensing effect of cholesterol. The picture is changed completely in the latter case: here, cholesterol enhances rotational motion. The enhancement may be explained by taking into account that beyond the bulky steroid nucleus, more freedom for motion exists.

Because this explanation is based on the topological properties of the cholesterol-containing bilayers only, the found property probably may be important for physiological temperatures, as well. In particular, it may imply that cholesterol weakens interaction between the two leaflets in the bilayer.

Acknowledgment. This work was supported by the Russian Foundation for Basic Research, Grant no. 08-03-00261, by the Ministry of Education and Science of the Russian Federation, project no. 2.1.1/1522, and by the Siberian Branch of RAS, project no. 75.

References and Notes

(1) Bloom, M.; Evans, E.; Mouritsen, O. G. *Q. Rev. Biophys.* **1991**, *24*, 293–397.
(2) Endress, E.; Bayerl, S.; Prechel, K.; Maier, C.; Merkel, R.; Bayerl, T. M. *Langmuir* **2002**, *18*, 3293–3299.
(3) Needman, D.; Nunn, R. S. *Biophys. J.* **1990**, *58*, 997–1009.
(4) Henriksen, J. R.; Rowat, A. C.; Ipsen, J. H. *Eur. Biophys. J.* **2004**, *33*, 732–741.
(5) Thewalt, J. L.; Bloom, M. *Biophys. J.* **1992**, *63*, 1176–1181.
(6) Henriksen, J.; Rowat, A. C.; Brief, E.; Hsueh, Y. W.; Thewalt, J. L.; Zuckermann, M. J.; Ipsen, J. H. *Biophys. J.* **2006**, *90*, 1639–1649.
(7) Urbina, J. A.; Pekerar, S.; Le, H. B.; Patterson, J.; Montez, B.; Oldfield, E. *Biochim. Biophys. Acta* **1995**, *1238*, 163–176.
(8) Hofsäss, C.; Lindahl, E.; Edholm, O. *Biophys. J.* **2003**, *84*, 2192–2206.
(9) Hung, W.-C.; Lee, M.-T.; Chen, F.-Y.; Huang, H. W. *Biophys. J.* **2007**, *92*, 3960–3967.
(10) Czech, M. P. *Nature* **2000**, *407*, 147–148.
(11) Veatch, S. L.; Keller, S. L. *Phys. Rev. Lett.* **2002**, *89*, 268101.
(12) Simons, K.; Ikonen, E. *Nature* **1997**, *387*, 569–572.
(13) Karp, G. *Cell and Molecular Biology: Concepts and Experiments*, 4th ed.; John Wiley & Sons: New York, 2004; Chapter 4.
(14) Filippov, A.; Oradd, G.; Lindblom, G. *Langmuir* **2003**, *19*, 6397–6400.
(15) Kurad, D.; Jeschke, G.; Marsh, D. *Biophys. J.* **2004**, *86*, 264–271.
(16) Chachaty, C.; Rainteau, D.; Tessier, C.; Quinn, P. J.; Wolf, C. *Biophys. J.* **2005**, *88*, 4032–4044.
(17) Ghimire, H.; Inbaraj, J. J.; Lorigan, G. A. *Chem. Phys. Lipids* **2009**, *160*, 98–104.
(18) Isaev, N. P.; Dzuba, S. A. *J. Phys. Chem. B* **2008**, *112*, 13285–13291.
(19) Isaev, N. P.; Kulik, L. V.; Kirilyuk, I. A.; Reznikov, V. A.; Grigor'ev, I. A.; Dzuba, S. A. *J. Non-Cryst. Solids* **2010**, *356*, 1037–1042.
(20) Isaev, N. P.; Syryamina, V. N.; Dzuba, S. A. *Appl. Magn. Reson.* **2010**, *37*, 405–413.
(21) Dzuba, S. A. *Phys. Lett. A* **1996**, *213*, 77–84.
(22) Erilov, D. A.; Bartucci, R.; Guzzi, R.; Marsh, D.; Dzuba, S. A.; Sportelli, L. *J. Phys. Chem. B* **2004**, *108*, 4501–4507.
(23) Erilov, D. A.; Bartucci, R.; Guzzi, R.; Marsh, D.; Dzuba, S. A.; Sportelli, L. *Biophys. J.* **2004**, *87*, 3873–3881.
(24) Bartucci, R.; Erilov, D. A.; Guzzi, R.; Sportelli, L.; Dzuba, S. A.; Marsh, D. *Chem. Phys. Lipids* **2006**, *141*, 142–157.
(25) Toropov, Y. V.; Dzuba, S. A.; Tsvetkov, Y. D.; Monaco, V.; Formaggio, F.; Crisma, M.; Toniolo, C.; Raap, J. *Appl. Magn. Reson.* **1998**, *15*, 237–246.
(26) Salikhov, K. M.; Dzuba, S. A.; Raitsimring, A. M. *J. Magn. Reson.* **1981**, *42*, 255–276.
(27) Weisz, K.; Gröbner, G.; Mayer, C.; Stohrer, J.; Kothe, G. *Biochemistry* **1992**, *31*, 1100–1112.
(28) Lehnert, R.; Eibl, H.-J.; Müller, K. *J. Phys. Chem. B* **2004**, *108*, 12141–12150.
(29) Subczynski, W. K.; Wisniewska, A.; Hyde, J. S.; Kusumi, A. *Biophys. J.* **2007**, *92*, 1573–1584.
(30) Dufourc, E. J.; Parish, E. J.; Chitrakom, S.; Smoth, I. C. P. *Biochemistry* **1984**, *23*, 6062–6071.
(31) Levine, Y. K.; Wilkins, M. H. *Nat. New Biol.* **1971**, *230*, 69–72.
(32) McIntosh, T. J. *Biochim. Biophys. Acta* **1978**, *513*, 43–58.
(33) Worcester, D. L.; Franks, N. P. *J. Mol. Biol.* **1976**, *100*, 359–378.
(34) Rappolt, M.; Vidal, M. F.; Kriechbaum, M.; Steinhart, M.; Amenitsch, H.; Bernstorff, S.; Laggner, P. *Eur. Biophys. J.* **2003**, *31*, 575–585.
(35) Pencer, J.; Nieh, M. P.; Harroun, T. A.; Krueger, S.; Adams, C.; Katsaras, J. *Biochim. Biophys. Acta* **2005**, *1720*, 84–91.
(36) Hung, W.-C.; Lee, M.-T.; Chen, F.-Y.; Huang, H. W. *Biophys. J.* **2007**, *92*, 3960–3967.
(37) Wagner, A. J.; Loew, S.; May, S. *Biophys. J.* **2007**, *93*, 4268–4277.
(38) Putzel, G. G.; Schlick, M. *Biophys. J.* **2008**, *94*, 869–877.
(39) Collins, M. D. *Biophys. J.* **2008**, *94*, L32–L34.

JP1043927